Resonant tunneling in submicron double-barrier heterostructures

Bo Su and V. J. Goldman
Department of Physics, State University of New York, Stony Brook, New York 11794-3800

M. Santos and M. Shayegan
Department of Electrical Engineering, Princeton University, Princeton, New Jersey 08544

(Received 15 October 1990; accepted for publication 10 December 1990)

We have fabricated submicron resonant tunneling devices from double-barrier AlGaAs/GaAs heterostructures using electron beam lithography and wet chemical etching. These devices exhibit step-like features in the current-voltage curves. We interpret these steps as arising from additional size quantization of the electronic states in the well due to in-plane lithographic confinement. Magnetotunneling experiments on these devices are reported for the first time. A simple model calculation describes well the experimental data.

Double-barrier resonant tunneling structures (DBRTS) provide appealing experimental systems for studying low-dimensional phenomena. The electronic states between the two barriers in the well are two-dimensional (2D).[1] Additional lateral confinement can be achieved by surface depletion of the etching wall for small devices made by microfabrication techniques ("quantum dots").[2-6] Such three-dimensional confinement in a DBRTS can produce zero-dimensional (0D) states in the well as has been observed by Reed *et al.*[3,5] In their case, however, device of about 100 nm in diameter is pinched off completely (at zero bias) by surface depletion so that there is a shift of the position of the resonant current peak compared with the large-area devices.

In this letter we report our results on submicron DBRTS devices, which are not pinched off completely, that is, there is an undepleted area in the doped emitter electrode. These devices exhibit step-like current-voltage (I-V) curves which result in a set of peaks in the differential conductance curves. We interpret this behavior as due to resonant tunneling through the discrete 0D electronic states in the well produced by the in-plane confinement.

Our DBRTS was grown by molecular beam epitaxy on a n^+ ⟨100⟩GaAs substrate. In order of growth the layers are: (1) 500 nm GaAs doped with Si to 2.2×10^{17} cm^{-3}, (2) 10 nm undoped GaAs spacer, (3) 8.5 nm undoped $Al_{0.50}Ga_{0.50}As$ (higher barrier), (4) 5.6 nm undoped GaAs (well) (5) 8.5 nm undoped $Al_{0.40}Ga_{0.60}As$ (lower barrier), (6) 5 nm undoped GaAs spacer, (7) 500 nm GaAs doped with Si to 2.2×10^{17} cm^{-3}. Devices were defined by electron beam lithography and wet chemical etching. Au-Ni-Ge circular dots serve as self-aligned mesa-etching masks. Good ohmic contacts were obtained by alloying the devices in a N_2-H_2 atmosphere at 300 °C for about 50 s.

Figure 1 gives the I-V characteristic for a large-area device which has a Au-Ni-Ge contact pad diameter $D = 2.8$ μm. The resonant current has a peak of 33 nA at $V_p \simeq 246$ mV in the positive bias.[7] This device exhibits peak-to-valley (PTV) current ratio of about 25:1, which indicates that our lithographic process does not induce appreciable device quality degradation. The ratio of the peak currents in positive and negative bias polarities is 1:7, reflecting the asymmetric design of the barriers in the wafer.[8] Under negative bias, electrons tunnel from the emitter into the well through the lower barrier and leave the well through the higher collector barrier; the electron density in the well is high enough to cause bistability between -373 and -404 mV.[9] Under positive bias, electrons from the emitter tunnel into the well through higher barrier and leave the well by tunneling through lower barrier; the electron density in the well is considerably lower than that under negative bias and the voltage shift caused by the electronic charge stored in the well is small. We will focus on the positive bias regime for small-area devices for this reason.

Figure 2 shows dI/dV as a function of voltage in the positive bias for several sizes D of devices. A weak, but quite reproducible structure in the dI/dV vs V curves is observable even in devices as large as $D = 2$ μm. For yet smaller D the structure becomes stronger. The I-V characteristic of our smallest device, which has contact pad diameter $D = 0.6$ μm, is shown in Fig. 3 (positive bias only). Between threshold voltage $V_{th} \simeq 120$ mV and $V_p \simeq 223$ mV, the step-like structure is clearly seen in the I-V curve (this structure starts to wash out at $T \simeq 10$ K and completely disappears at 77 K). The device has a PTV current ratio of 3:1, which is considerably less than that of

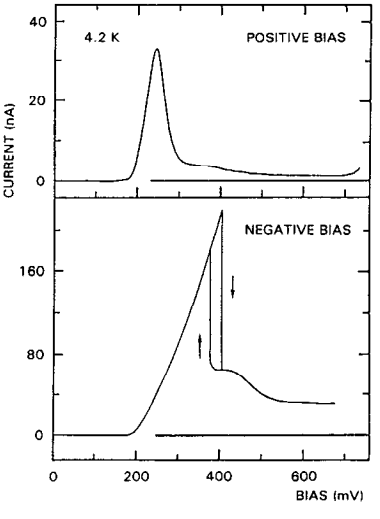

FIG. 1. I-V curve of a large-area device ($D = 2.8$ μm) at 4.2 K. The asymmetry of the I-V curve for positive/negative bias is due to the asymmetry in the barrier material composition (height).

 0003-6951/91/070747-03$02.00

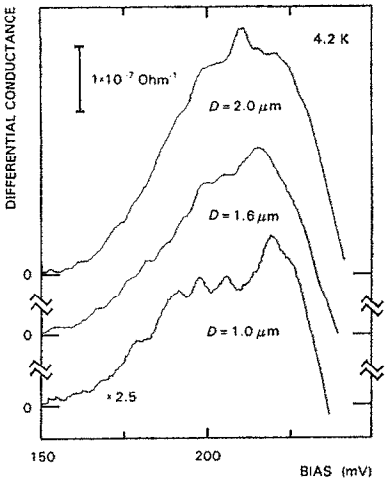

FIG. 2. dI/dV vs V curves (positive bias only) for three different size devices, where D is the Au-Ni-Ge contact (etching mask) diameter. The structure in the differential resistance is due to lateral size quantization.

the large-area devices.[10] The peak current is about 90 pA at $V_p \simeq 223$ mV; V_p is close to that of the large-area devices. This shows that our device is *not* completely pinched off by surface depletion. The undepleted core has a diameter (defined as $2r_o$) of about 150 nm, which is obtained by scaling the peak current.[11] The etching undercut and surface depletion are responsible for the difference between D and $2r_o$.

In large-area DBRTS devices, the 2D states in the well form a continuous subband. Because of the lateral confinement imposed by the etching wall in small devices, the states in the well become discrete energy levels. The energy difference between two adjacent levels is determined, partly, by the size of the undepleted core of radius r_o. For $V < V_{th}$, the lowest discrete energy level (the ground state)

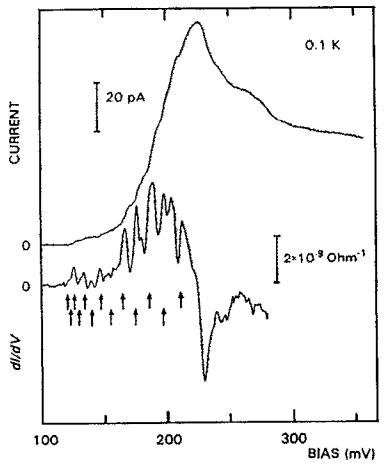

FIG. 3. I-V and dI/dV vs V curves (positive bias) for the $D = 0.6$ μm device. The arrows give the positions of the peaks in dI/dV vs V calculated from the model described in the text. The upper row are the $m = 0$ states and the lower row are the $m = 1$ states. From left to right, $n = 1,2,3\ldots$.

in the well is above the Fermi energy E_F in the emitter (E_F is about 20 mV in our devices). Because of the heavy doping, we assume that the density of states in the emitter has the same 3D character as in the large-area devices.

When the ground state in the well matches E_F in the emitter, the resonant tunneling sets in. As V increases further, the tunneling current does not change rapidly until the next level in the well crosses E_F in the emitter when I makes the next step up. This process results in a step-like I-V curve and continues until the ground state in the well passes the bottom of the conduction band in the emitter. For higher V, states with the in-plane momentum larger than the Fermi momentum $\hbar k_F$ in the emitter cross E_F in the emitter. Therefore, resonant tunneling of electrons conserving both energy and the in-plane momentum is no longer possible.[10,12]

The lower trace in Fig. 3 gives dI/dV vs V. The structure in the I-V curve presents itself much more clearly as a series of peaks in the derivative data. The peaks in the dI/dV trace occur when the I-V curve steps up, that is, when a state in the well is aligned with E_F in the emitter. Figure 4(a) gives dI/dV as a function of V in relatively weak magnetic field applied parallel to the tunneling direction. The data is complex, but the general features of the curves resemble that of the $B = 0$ curve. Figure 4(b) shows the dI/dV vs V data taken in strong magnetic field. The strong B curves are very different from the $B = 0$ curve. Two energies are relevant in magnetic field; one is the Landau level separation $\hbar\omega_c$ and the other is the energy difference δE between two discrete levels in the well ($\hbar\omega_c = 1.7$ meV/T and the δE is typically 3–5 meV). In relatively weak B, $\hbar\omega_c$ is smaller than δE. The Zeeman splitting of degenerate states in the well is small compared to δE, and although the Zeeman-split states move to higher and lower bias from the unsplit levels, the general character of the data is not affected. In strong B the electrons in the emitter occupy only the lowest $N = 0$ Landau level (extreme quantum limit) while the Zeeman splitting of the levels in the well is greater than δE. Thus one would expect to see quite different features in the dI/dV vs V curves in strong B.

In order to gain a better understanding of our devices we develop a model, which is essentially a 3D (emitter) to 0D (the confined well) to 3D (collector) incoherent resonant tunneling model.

Consider the confined well region. It is a cylindrical slab defined by the two barriers and the depleted sidewall of the etching surface. In the hard wall approximation we can write the Schroedinger equation and the boundary condition for an electron in cylindrical coordinates (r, ϕ, z) as follows:

$$(-\hbar^2/2m^*)\nabla^2\Psi = E\Psi \tag{1}$$

and

$$\Psi(r = r_o) = 0, \tag{2}$$

where Ψ is the electron wave function and m^* is its effective mass in GaAs. We can solve Eq. (1) by separating variables as $\Psi = R\Phi Z$. In the z direction the energy eigen-

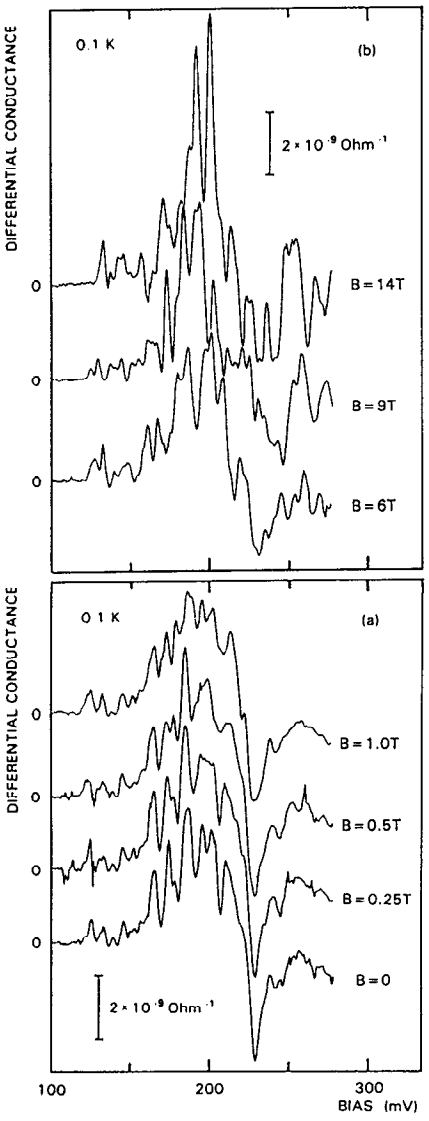

FIG. 4. dI/dV vs V curves for the $D = 0.6$ μm device of Fig. 3 in a magnetic field parallel to the tunneling direction.

value is the same as for large-area devices, $E_z = E_o$, where E_o is the bottom of the lowest subband in the well (for our DBRTS $E_o \simeq 80$ meV). The other two solutions of Eq. (1) have the form:

$$\Psi = \exp(im\phi), \tag{3}$$

and

$$R = J_m(kr), \tag{4}$$

where m is a nonnegative integer, J_m are Bessel functions, and $(\hbar k)^2 = 2m^*(E - E_o)$. Using the boundary condition (2) we have:

$$E_{n,m} = E_o + (\hbar^2/2m^*)(X_{n,m}/r_0)^2, \tag{5}$$

where $X_{n,m}$ is the n th root of $J_m(X) = 0$; n and m are the principal and orbital (angular momentum) quantum numbers, respectively. The arrows in Fig. 3 indicate the positions of peaks giving the energy levels determined from Eq. (5) where E_o was taken to give correctly the position of the first level. In the conversion of the energies to voltages we have neglected the space charge in the well, since in the positive bias polarity it is small, as discussed above. The only other device-dependent quantity, r_0, is taken to equal the conducting core radius, calculated from the values of the peak current of the device and the current density for large-area devices close (on the DBRTS wafer) to present device.

The energy levels given by Eq. (5) have two interesting properties. First, for $n > 3$ there is a considerable *near degeneracy* of the levels given by $E_{n+1,m} \cong E_{n,m+2}$. This near degeneracy reduces the number of observable differential resistance peaks and makes some of them stronger than others. Second, the energy difference between the adjacent series of the nearly degenerate levels increases linearly with n. This explains the fact that the effect of confinement is observable even in devices as large as $D = 2$ μm. We note that the geometry of the device enters the model as the boundary condition (2). It is very difficult to know the geometry of the undepleted core of device, but, because of the electrostatic nature of the surface depletion, it is not expected to contain any sharp corners so that a circular cross section appears to be a good approximation.

[1] L. L. Chang, L. Esaki, and R. Tsu, Appl. Phys. Lett. **24**, 593 (1974).
[2] K. Kash, A. Scherer, J. M. Worlock, H. G. Craighead, and M. C. Tamargo, Appl. Phys. Lett. **49**, 1043 (1986).
[3] M. A. Reed, J. N. Randall, R. J. Aggarwal, R. J. Matyi, T. M. Moore, and A. E. Wetsel, Phys. Rev. Lett. **60**, 535 (1988).
[4] T. P. Smith III, K. Y. Lee, C. M. Knoedler, J. M. Hong, and D. P. Kern, Phys. Rev. B **38**, 2172 (1988).
[5] M. Luban, J. H. Luscombe, M. A. Reed, and D. L. Pursey, Appl. Phys. Lett. **54**, 1997 (1989).
[6] S. Tarucha, Y. Hirayama, T. Saku, and T. Kimura, Phys. Rev. B **41**, 5459 (1990).
[7] The bias polarity is with respect to the substrate.
[8] A. Zaslavsky, V. J. Goldman, D. C. Tsui, and J. E. Cuningham, Appl. Phys. Lett. **53**, 1408 (1988).
[9] V. J. Goldman, D. C. Tsui, and J. E. Cuningham, Phys. Rev. Lett. **58**, 1256 (1987).
[10] The PTV ratio always becomes smaller in smaller size devices (for $D \leqslant 2$ μm). While this phenomenon is not fully understood at present, it is not related to processing damage since it occurs also in chemically etched devices with nonalloyed contacts [K. W. Goossen et al., IEDM 89 (1989)]. Since the reduction of the PTV ratio sets in at the same D at which the I-V curves start to show the lateral quantization structure, it appears that the two phenomena are related. The likely origin of the rise of the valley current is the Heisenberg uncertainty principle, which requires that the in-plane momentum of a tunneling electron has an uncertainty of $\simeq \hbar/r_o$. The uncertainty in the in-plane momentum relaxes the requirement of the conservation of the in-plane component of the momentum which gives rise to a valley current in a manner similar to the ionized impurity scattering.
[11] For large-area devices the peak current I_p is the product of peak tunneling current density, J_p, and the device area (J_p does not change with area). We assume it is also true for smaller devices so long as the emitter electrode contains an undepleted region.
[12] S. Luryi, Appl. Phys. Lett. **47**, 490 (1985)].